



Cite this: *Polym. Chem.*, 2024, **15**, 3657

## CO<sub>2</sub>-based polycarbonates from biobased cyclic terpenes with end-of-life usage potential†

Philipp Holzmüller,<sup>a</sup> Jasmin Preis<sup>b</sup> and Holger Frey<sup>ID, \*a</sup>

Biobased polymers have garnered increasing attention in recent years, aiming at more sustainable materials. This study focuses on the synthesis of polycarbonates sourced from cyclic terpenoid-based monomers and CO<sub>2</sub>, representing polymers derived from a biobased feedstock. Menthyl, thymyl, and carvacryl glycidyl ethers, synthesized from menthol, thymol, and carvacrol and epichlorohydrin were copolymerized with CO<sub>2</sub> using catalytic systems such as (R,R)-(salicy)-Co(III)Cl (Co(Salen)Cl) and bis(triphenylphosphine)-iminium chloride ([PPN]Cl) or triethylborane (TEB)/[PPN]Cl. Moderate to high molar mass polymers (up to 60 kg mol<sup>-1</sup>) were obtained with low dispersities ( $M_w/M_n < 1.24$ ) via solvent-free bulk copolymerization. Despite the sterically demanding nature of these monomers, the cobalt-based catalyst system exhibited high monomer conversion, polymer selectivity, and carbonate linkage content. The resulting polycarbonates exhibited glass transition temperatures ( $T_g$ ) ranging from 41 to 58 °C, when the polymer backbone consisted solely of polycarbonate linkages. However, with decreasing polycarbonate linkage content, the  $T_g$  value dropped to 0 °C for the menthol based polycarbonate. The aromatic side chain polycarbonates displayed not only the highest  $T_g$  values, but also the highest thermal stability, with  $T_{5\%}$  reaching 260 °C. The thymol-based polycarbonate exhibited a Young's modulus ( $E$ ) of  $645 \pm 43$  MPa and an elongation at break ( $\epsilon$ ) of  $5 \pm 2\%$ , as determined by tensile testing. All three biobased polymers underwent complete degradation under strong basic conditions (5 M KOH) within 30 hours, yielding their respective diols and CO<sub>2</sub>, thus offering potential for end-of-life usage. CO<sub>2</sub> generated by thermal decomposition can be recycled for copolymerization, while the diols could find application for other purposes.

Received 18th July 2024,  
Accepted 26th August 2024  
DOI: 10.1039/d4py00797b  
[rsc.li/polymers](http://rsc.li/polymers)

## Introduction

The United Nations (UN) launched the Sustainable Development Goals (SDGs) initiative in 2015, aiming at universal guidelines for achieving fair and responsible development while preserving the well-being of both humanity and ecosystems.<sup>1</sup> This initiative comprises a targeted agenda to be achieved by 2030, consisting of 17 goals and 169 targets focused on promoting economic growth, environmental conservation, social equity, and human welfare.<sup>2</sup> Biobased polymers emerge as significant contributors to achieving the SDGs, particularly objectives related to "Responsible

Consumption and Production", "Clean Water and Sanitation", and "Life on Land".<sup>3</sup> Established polycarbonates, derived from bisphenol A (BPA), are widely used as thermoplastic polymers renowned for their toughness, impact resistance, and optical clarity, making them prevalent in medical, optical, and electronic applications.<sup>4</sup> However, polycarbonates based on BPA and phosgene pose toxicity risks due to the release of hazardous volatile compounds, particularly when utilized in food containers.<sup>5</sup> An alternative approach to produce more sustainable polycarbonates is the utilization of CO<sub>2</sub> and epoxides, employing ring opening copolymerization (ROCP).<sup>6,7</sup> For instance, poly(propylene carbonate) (PPC), obtained by copolymerizing CO<sub>2</sub> and propylene oxide (PO), represents a polycarbonate with high CO<sub>2</sub> content and is produced on industrial-scale.<sup>8</sup> Additionally, this polycarbonate route offers the possibility to use the greenhouse gas CO<sub>2</sub> as C1 building block, contributing to carbon capture and usage.<sup>9</sup> However, the synthesis of PO and therefore also PPC still relies on fossil resources. Consequently, there is a growing interest in developing nature-based polycarbonates relying on biobased epoxides and CO<sub>2</sub>, offering a more sustainable alternative to achieve the SDGs.

<sup>a</sup>Department of Chemistry, Johannes Gutenberg University Mainz, Duesbergweg 10-14, 55128 Mainz, Germany. E-mail: [hfrey@uni-mainz.de](mailto:hfrey@uni-mainz.de)

<sup>b</sup>PSS Polymer Standards Service GmbH, In der Dalheimer Wiese 5, 55120 Mainz, Germany

† Electronic supplementary information (ESI) available: Detailed information on reagents, instrumentation, experimental and synthetic methods. Characterization of all monomers, copolymers, (NMR, SEC, DSC, MALDI-ToF). Retrosynthesis of presented bio-based polymers. See DOI: <https://doi.org/10.1039/d4py00797b>



Various natural sources such as phenylpropanoids,<sup>10</sup> sugars,<sup>11</sup> castor oil,<sup>12</sup> fatty acids,<sup>13</sup> and notably terpenes<sup>14</sup> have been utilized for  $\text{CO}_2$  based polycarbonate synthesis. One prominent example is poly(limonene oxide) carbonate (PLimC), derived from limonene oxide (LO) and  $\text{CO}_2$ . Several authors have suggested scalability of PLimC production and its suitability for applications like gas separation membranes due to its permeability and film-forming properties.<sup>15–17</sup> Moreover, PLimC can be post-modified to achieve and tailor a variety of polymer properties, including antibacterial, sea water solubility, or rubber-like properties.<sup>17</sup> However, a limitation arises as only a few catalysts, primarily zinc-based compounds, have shown efficacy in polymerizing limonene oxide. Consequently, other structurally demanding terpene-based polycarbonates have been explored, utilizing monomers such as menth-2-ene oxide<sup>18</sup> and pinene oxide.<sup>19</sup>

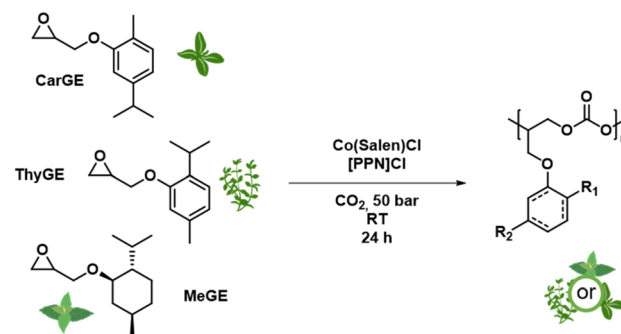
These terpene-based monomers face challenges in terms of specific catalysts requirements and epoxide synthesis, often requiring multistep syntheses. For instance, in the case of limonene oxide (LO) synthesis for ROCOP, selective *trans*-LO synthesis is usually necessary. Recently, long-chain terpene-based polycarbonates derived from citronellyl glycidyl ether<sup>20</sup> and geranyl glycidyl ether<sup>21</sup> have been published by our group. The monomers were synthesized in one-step reactions from the respective alcohols and epichlorohydrin (ECH) and require simple purification *via* distillation. Traditionally, ECH is produced through a multi-step process involving propylene and chlorine, which is not considered highly sustainable due to the use of chlorine.<sup>22,23</sup> However, ECH can also be derived from triacylglycerol *via* the Epicerol process.<sup>23–25</sup> The bio-sourcing of ECH from glycerol is particularly sustainable when glycerol is obtained as a byproduct from biodiesel production.<sup>26</sup> While this synthesis route for ECH is more sustainable, ECH itself must still be handled with care and within closed environments.

However, these long-chain terpene-based polymers exhibit  $T_g$  values below  $-29^\circ\text{C}$ , making them unsuitable for usage as potential thermoplastic materials like PLimC. Nonetheless, the class of terpenes offers a wide range of structures, comprising more than 30 000 variants with linear, cyclic, or multicyclic configurations.<sup>27</sup> From a polymer point of view, cyclic terpenes are of particular interest as their molecular structure is rather rigid. This is expected to result in polymers with potentially enhanced glass temperatures, rendering them suitable for applications as engineering plastics.<sup>28</sup> Some of the simplest cyclic terpenoid structures suitable for monomer synthesis with ECH include carvacrol, thymol, and menthol. They can be extracted from oregano,<sup>29</sup> thyme,<sup>30</sup> and mint,<sup>31</sup> respectively, but can also be produced in bioreactors.<sup>32</sup> These terpenoids find extensive application in the pharmaceutical industry, particularly due to their antioxidant, antiseptic, antibacterial, antifungal, and antimicrobial properties.<sup>33</sup> In polymer chemistry, carvacrol, thymol, and menthol have been utilized especially for polymer blends in which these terpenoids enhanced the bioactivity/bioresistance of the polymers or the polymers acted as host material to slowly release these ter-

noids.<sup>34</sup> However, carvacrol, thymol, and menthol derivatives have also been polymerized to polyamides,<sup>35</sup> polyesters,<sup>36</sup> polyacrylates,<sup>37</sup> polybenzoxazines,<sup>38</sup> polyphenols,<sup>39</sup> with menthol being the only one used for polycarbonate synthesis recently.<sup>18</sup>

Another issue to consider when discussing biobased polycarbonates in the context of fulfilling the SDGs is their end-of-life usage. In recent years, there has been increasing attention given to the degradation and recycling of polymers to enable a circular economy.<sup>40</sup> Various strategies have been explored in the field of  $\text{CO}_2$ -based polycarbonates to achieve circularity.<sup>41</sup> For instance, polycarbonates can undergo solvolysis under acidic or basic conditions yielding in the corresponding diols and  $\text{CO}_2$ .<sup>42</sup> In such cases, the toxicity and potential reuse options of the resulting molecules need to be carefully evaluated. Additionally,  $\text{CO}_2$ -based polycarbonates can be degraded to their respective cyclic carbonates *via* catalysis,<sup>43</sup> which can then be repurposed for applications such as green solvents or electrolytes in batteries.<sup>44</sup> Chemical recycling to monomers (CRM) for  $\text{CO}_2$ -based polycarbonates has also garnered increasing attention in recent years due to its potential for full circularity.<sup>45,46</sup> Thereby, the focus is on the straightforward and efficient recovery of the respective epoxide and  $\text{CO}_2$  using a catalytic system.<sup>47</sup> For terpene-based polycarbonates, only studies for poly(limonene oxide) carbonate (PLimC) have been conducted, aiming at achieving CRM and demonstrating degradability in anaerobic environments.<sup>48</sup>

In this study, we present the copolymerization of different biobased cyclic terpenyl glycidyl ethers with  $\text{CO}_2$  to produce polycarbonates. Our main focus was on extending the platform of terpene-based polycarbonates. We successfully synthesized a range of copolymers based on carvacryl glycidyl ether (CarGE), thymyl glycidyl ether (ThyGE) and menthyl glycidyl ether (MeGE) (see Scheme 1). Different parameters like catalyst loading, catalytic system, solvents and chain transfer agents were varied to investigate the effect on the copolymerization with  $\text{CO}_2$ . The resulting polymers were analysed regarding their material properties like glass temperature, thermal stability and mechanical performance. We also investigated polymer degradation under basic conditions and the possible usage of the degradation products.



**Scheme 1** Synthesis of cyclic terpenoid-based polycarbonates.



## Results and discussion

### Monomer synthesis

The terpenoid-based epoxides investigated in this study were prepared using a Williamson ether synthesis approach. This method involves reaction of the respective terpenoid alcohol with ECH. We adapted a method known for similar epoxide structures to achieve high yields of up to 89% of the phenyl-based terpenoids.<sup>49</sup> The menthol-based epoxide, synthesized according to patent literature, was obtained in yields up to 74%.<sup>50</sup>

To the best of our knowledge, none of the resulting epoxides – CarGE, ThyGE, or MeGE – has been previously utilized in any polymerization process. Demonstrating scalability, we synthesized all epoxide monomers on a 50 g scale and efficiently purified them *via* vacuum distillation (see ESI† for detailed methods). ECH can be obtained from triacylglycerol *via* the Epiceral process (see ESI Schemes S1 and S2†).<sup>23–25</sup> To ensure the absence of protic impurities in the monomer, all epoxides were treated with iodomethane and sodium hydride, achieving quantitative yields. This method not only prevents catalyst deactivation, but also minimizes additional polymer initiation by alcohols, ultimately enhancing the polymers' molar masses and dispersities.<sup>15</sup> The successful synthesis of all terpenoid-based epoxides was verified by <sup>1</sup>H and <sup>13</sup>C NMR spectroscopy (see ESI Fig. S1–S6†). The <sup>1</sup>H NMR spectrum of CarGE (Fig. 1) illustrates the characteristic epoxide signals highlighted in blue. Comparison of the <sup>1</sup>H NMR peaks of the bulky side chain (in green) reveals a marginal variation among the alcohol, monomer, and polymer. However, specific peaks for epoxide and polycarbonate can be identified.

### Copolymerization of CarGE with CO<sub>2</sub>

CarGE was chosen for in-depth copolymerization analysis due to a less sterically demanding structure compared to the other monomers. CarGE and CO<sub>2</sub> were copolymerized in bulk using Co(Salen)Cl and [PPN]Cl as catalysts, employing 50 bar at room temperature for 24 hours, see Table 1 (detailed pro-

cedure in the ESI†). The catalytic system was chosen because of its known high tolerance for sterically demanding monomers like cyclohexene oxide and other glycidyl ethers.<sup>51</sup> 50 bar CO<sub>2</sub> pressure was chosen as standard operating pressure because this binary catalyst demonstrates best performance under high CO<sub>2</sub> pressure.<sup>10</sup> The copolymerization was stopped by releasing the excess CO<sub>2</sub>, and the success of the copolymerization was primarily assessed *via* <sup>1</sup>H NMR spectra determining the selectivity towards polymer formation (see ESI Fig. S20†). In the case of CarGE copolymerization, small traces of cyclic carbonates were identified, indicating a selectivity towards the formation of polycarbonate despite its demanding side chain compared to monomers like propylene oxide (PO). The noticeable side chain structure does not facilitate backbiting of the chain end, resulting in no observable differences compared to PO.<sup>52</sup> The polymers were purified by precipitation in methanol, reaching yields up to 86%. Verification of the successful polycarbonate synthesis was achieved by <sup>1</sup>H NMR and <sup>13</sup>C NMR characterization of the isolated polymer, in which the typical proton signals of the CO<sub>2</sub>/epoxide based polycarbonate backbone were identified at 5.20 and 4.50 ppm (see ESI Fig. S7 and S8†). Furthermore the selectivity towards polycarbonate linkages was investigated *via* <sup>1</sup>H NMR characterization to ensure a low content of polyether defects. The Co(Salen)Cl catalyst showed high selectivity for polycarbonate linkages, consistently yielding polycarbonate linkages exceeding 99%. Optimization of the monomer: initiator: catalyst ratio was pivotal in achieving high molar masses of the resulting PCarGEC while minimizing the catalyst loading. Entries 1–7 in Table 1 illustrate that the highest  $M_n$  can be achieved with a monomer: initiator: catalyst ratio of 2000:2:2, resulting in a  $M_n$  of 59.5 kg mol<sup>−1</sup> with a dispersity ( $D$ ) of 1.15, determined *via* size exclusion chromatography with THF as an eluent and polystyrene standards (SEC, THF, PS). The ratio of catalyst to co-catalyst (initiator) was always maintained at 1:1, based on investigations for this system that revealed this ratio performs best.<sup>53</sup> Despite efforts to reduce the water content in the reac-

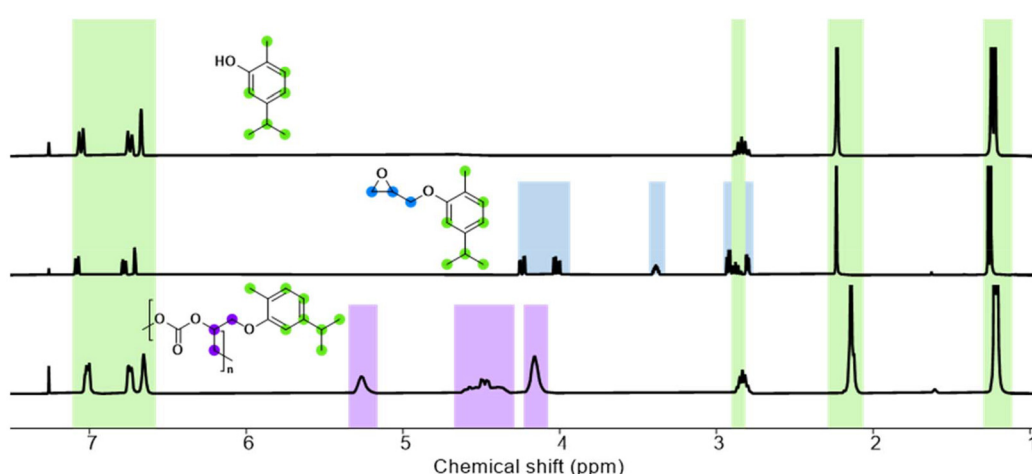


Fig. 1 <sup>1</sup>H NMR spectra of carvacrol, CarGE and PCarGEC, measured in CDCl<sub>3</sub>.



**Table 1** Copolymerization of CarGE with CO<sub>2</sub> for different catalysts and catalyst loading ratios

Entry	Catalyst	[m] <sub>0</sub> : [i] <sub>0</sub> : [cat] <sub>0</sub> <sup>a</sup>	Conv. <sup>b</sup> (%)	Select. <sup>c</sup> (%)	PC <sup>d</sup> (%)	M <sub>n</sub> <sup>e</sup> (D) (kg mol <sup>-1</sup> )	T <sub>g</sub> (°C)
1	Co(Salen)Cl	2000 : 8 : 8	100	92	>99	20.5 (1.13)	48
2	Co(Salen)Cl	2000 : 5 : 5	100	93	>99	35.8 (1.12)	48
3	Co(Salen)Cl	2000 : 4 : 4	100	94	>99	43.8 (1.10)	48
4	Co(Salen)Cl	2000 : 3 : 3	99	93	>99	50.0 (1.13)	49
5	Co(Salen)Cl	2000 : 2.5 : 2.5	98	93	>99	53.1 (1.13)	49
6	Co(Salen)Cl	2000 : 2 : 2	97	94	>99	59.5 (1.15)	49
7	Co(Salen)Cl	2000 : 1 : 1	38	86	>99	33.1 (1.15)	49
8	Co(Salen)Cl <sup>f</sup>	2000 : 14 : 4	100	81	>99	20.5 (1.12)	47
9	Co(Salen)Cl <sup>g</sup>	2000 : 3 : 3	96	92	>99	51.0 (1.12)	48
10	TEB	2000 : 2 : 4	35	0	—	—	—
11	TEB	2000 : 2 : 8	26	0	—	—	—
12	TEB	2000 : 2 : 16	62	22	80	11.9 (1.25)	37
13	TEB	2000 : 2 : 24	94	78	97	38.9 (1.13)	47

Reaction conditions: Co(Salen)Cl or TEB as a catalyst and [PPN]Cl as an initiator, monomer (1 mL), 50 bar CO<sub>2</sub>, r.t. (reaction with TEB at 60 °C), 24 hours. <sup>a</sup> [m]<sub>0</sub> = monomer equivalents, [i]<sub>0</sub> = initiator equivalents, [cat]<sub>0</sub> = catalyst equivalents. <sup>b</sup> Determined via <sup>1</sup>H NMR spectroscopy from the non-purified reaction mixture after opening the reactor; conv. = epoxide conversion determined via comparison of the relative integrals in the <sup>1</sup>H NMR spectrum of PC, CC, PE, and monomer. <sup>c</sup> Determined via <sup>1</sup>H NMR spectrum from the non-purified reaction mixture after opening the reactor; select. = polymer selectivity determined via comparison of the relative integrals in the <sup>1</sup>H NMR spectrum for PC against CC. <sup>d</sup> Determined via comparison of the relative integrals in the <sup>1</sup>H NMR spectrum for PC against PE. <sup>e</sup> Determined via SEC (THF, PS) and RI detector. <sup>f</sup> BDM was added as a CTA. The total concentration of [PPN]Cl and BDM is indicated as [i]<sub>0</sub>. [PPN]Cl and Co(Salen)Cl have the same ratio. <sup>g</sup> 0.3 mL toluene was added as solvent to the reaction mixture.

tion mixture (use of small reactor volumes and CO<sub>2</sub> storage over molecular sieve), bimodality in SEC curves persisted due to residual water traces in CO<sub>2</sub> (see Fig. 2). Furthermore, with lower initiator concentrations this bimodality was more dominant, which is due to increasing water/initiator ratios. Similar results were obtained for the recently published long chain terpenoid based polycarbonates by our group.<sup>21</sup> In general, the molar mass can be adjusted by varying the ratio of monomer, catalyst and initiator. Moreover, the addition of chain transfer agents (CTAs), *e.g.* 1,4-benzenedimethanol (BDM), to the reaction mixture allows to reach lower molar masses without higher catalyst loadings (see Table 1, entry 8). This is a common strategy for fine-tuning molar masses in polycarbonate synthesis.<sup>7,54</sup> Herein, BDM, acting as a bifunctional initiator, induces a shift in the SEC curve, transitioning from a

monofunctional-dominated bimodal curve to a strongly bimodal curve (see ESI Fig. S28†). SEC (THF, PS) was chosen as the standard analytical method for the polycarbonates, commonly used by most polycarbonate research groups. However, due to the significant structural differences between the CarGE based polycarbonate structure and the polystyrene standards used for SEC calibration, additional absolute molar mass determination was conducted. This was achieved by SEC with universal calibration in combination with intrinsic viscosity measurements as a well-known method.<sup>55</sup> Table S4† shows a discrepancy between the two absolute and relative methods, ranging between a 12–18% deviation, where the relative method consistently underestimates the molar mass. Therefore, the absolute molar mass for all CarGE-based polycarbonates is assumed to be higher than determined via SEC (THF, PS). When the catalyst loading is insufficient, both conversion and selectivity decrease within the 24 hour reaction time, resulting in lower molar masses as evidenced in Table 1, entry 7. For consistent comparison between various copolymerizations and their catalyst loadings, a fixed 24 hour time slot was consistently set. However, when reducing the reaction time to 6 hours for the monomer : initiator : catalyst ratio of 2000 : 2 : 2, 70% conversion was already achieved (see ESI Table S3†). Toluene was added as a solvent to the reaction mixture (see Table 1, entry 9) with the intention of improving bimodality/dispersity, as demonstrated in the literature.<sup>18</sup> After opening the reactor, the reaction mixture was slightly viscous but not solid, unlike the case without toluene. Comparing entries 4 and 9 in Table 1, no improvement in dispersity was observed, and molar mass, conversion, and polycarbonate linkages remained stable.

Independent of the chosen reaction conditions, the <sup>13</sup>C NMR spectra exhibit three peaks for the carbonate carbon, with one peak being notably dominant (see ESI Fig. S19†).

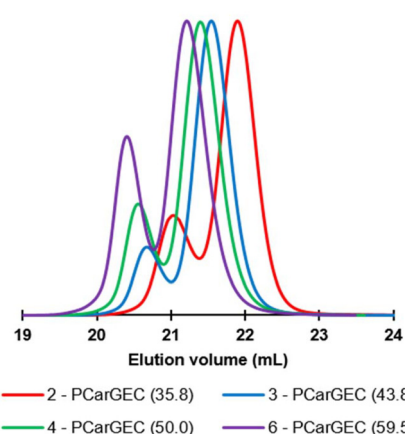


**Fig. 2** SEC traces of PCarGEC presented in Table 1 with different catalyst loading ratios (THF, PS, RI detector). M<sub>n</sub> of the respective polymers is shown in the legend.



This dominance indicates the prevalent formation of head-to-tail linkages, a characteristic behaviour of the Co(Salen)Cl/[PPN]Cl catalyst system.<sup>56</sup> To confirm the predominance of polycarbonate linkages in PCarGEC, MALDI-ToF characterization was employed, where the repeating unit matches the sum of epoxide units and CO<sub>2</sub> (see ESI Fig. S22†). All PCarGEC polymers show a glass temperature (*T<sub>g</sub>*) between 47 and 49 °C, with a slightly higher *T<sub>g</sub>* with higher molar masses. The Co(Salen)Cl/[PPN]Cl catalytic system poses challenges due to cobalt's environmental impact due to its mining.<sup>57</sup> In search of sustainable alternatives, attention has shifted to the metal-free catalyst triethylborane (TEB) in combination with the initiator [PPN]Cl.<sup>58</sup> In initial trials using this system to prepare PCarGEC, the epoxide:[PPN]Cl:TEB ratio was found to be pivotal for selective polycarbonate copolymerization. Entries 10–13 in Table 1 illustrate the copolymerization of CarGE with CO<sub>2</sub> by TEB catalysis, underscoring the critical role of selecting appropriate epoxide:[PPN]Cl:TEB ratios. The importance of these ratios was already reported in literature for the copolymerization of phenyl glycidyl ether with CO<sub>2</sub> to achieve the respective polycarbonate.<sup>59</sup> Here, insufficient TEB loading in the reaction mixture results in very low conversion and the formation of cyclic carbonates. With an increased TEB amount (Table 1, entry 12), conversion improves, but selectivity and content of polycarbonate linkages remain low. Only with a substantial TEB surplus, almost full conversion is achieved. Good selectivity, and high content of polycarbonate linkages are obtained, although not as high as with the cobalt-based system. Comparing the PCarGEC results with the copolymerization results of phenyl glycidyl ether and CO<sub>2</sub>, the more demanding structure of CarGE shows no worsening influence on polymerization selectivity.<sup>59</sup> A low ether linkage content in the polymer already affects the *T<sub>g</sub>* by decreasing it, as evidenced in Table 1, entry 13. Higher content of ether linkages increases this effect (Table 1, entry 12). A reaction temperature of 60 °C was necessary for all TEB catalysed copolymerizations, while lower temperatures did not induce any reaction. Regardless of the catalytic system and *M<sub>n</sub>* of the presented polymers, all PCarGECs exhibited long-term stability at room temperature or in the refrigerator without any autonomous post-polymerization modifications or degradation.

## Copolymerization of ThyGE and MeGE with CO<sub>2</sub>

We selected the thymol-based glycidyl ether ThyGE, a constitutional isomer of CarGE, for copolymerization to investigate the impact of the methyl/isopropyl group on the phenyl ring (Scheme 1). Additionally, we investigated the menthol-based glycidyl ether MeGE to see the effect of the phenyl ring in comparison to the cyclohexanyl ring. Furthermore, Wambach *et al.* recently reported the menthol-based polycarbonate poly(menth-2-ene carbonate) (PMen2C) as a terpene-based polymer.<sup>18</sup>

The herein presented menthol-based glycidyl ether induces higher chain flexibility compared to menth-2-ene oxide. In Table 2, the copolymerization of ThyGE or MeGE with CO<sub>2</sub> leads to results comparable to CarGE when using Co(Salen)Cl as a catalyst: mostly full conversion, high polymer selectivity, and high content of polycarbonate linkages. *M<sub>n</sub>* up to 60 kg mol<sup>-1</sup> with moderate dispersities was achieved. Similar to PCarGEC, these polymers display bimodality due to traces of water acting as initiator (see ESI Fig. S29†). Notably, PThyGEC and PMeGEC also showed an underestimation (13–18%) of the molar mass *via* SEC (THF, PS) (see ESI Table S4†). Both polycarbonate structures are confirmed by <sup>1</sup>H and <sup>13</sup>C NMR spectroscopy (see ESI Fig. S9–S12†) and MALDI-ToF characterization (see ESI Fig. S23 and S24†). After 6 hours of copolymerization, ThyGE and MeGE reached monomer conversions of 81% and 89%, respectively (see ESI Table S3†). The addition of toluene as a solvent to the reaction mixture does also not improve dispersities (see ESI Tables S1 and S2†). *M<sub>n</sub>* for both polymers can also be tuned by the addition of BDM (see ESI Tables S1 and S2†). The <sup>13</sup>C NMR indicates a slightly higher head-to-tail selectivity in both cases compared to PCarGEC (see ESI Fig. S19†). PThyGEC shows a *T<sub>g</sub>* of up to 58 °C, while the *T<sub>g</sub>* for PMeGEC reaches only 41 °C. MeGE and ThyGE are also copolymerizable with CO<sub>2</sub> by TEB catalysis. While the copolymerization of ThyGE shows similar results regarding polymer selectivity and content of carbonate linkages compared to CarGE (see Table S1†), MeGE afforded only polyether structures without any polycarbonate linkages with insufficient TEB loading (see Table S2†). Adjusting the TEB loading enabled an increase in polycarbonate linkages, albeit only up

**Table 2** Synthesis of ThyGE and MeGE based polycarbonates

Entry	Monomer	[m] <sub>0</sub> :[i] <sub>0</sub> :[cat] <sub>0</sub> <sup>a</sup>	Conv. <sup>b</sup> (%)	Select. <sup>c</sup> (%)	PC <sup>d</sup> (%)	<i>M<sub>n</sub></i> <sup>e</sup> (D) (kg mol <sup>-1</sup> )	<i>T<sub>g</sub></i> (°C)
1	ThyGE	2000:8:8	100	93	>99	27.9 (1.10)	55
2	ThyGE	2000:4:4	100	94	>99	48.0 (1.18)	57
3	ThyGE	2000:3:3	99	95	>99	60.0 (1.24)	58
4	MeGE	2000:8:8	100	95	>99	21.5 (1.11)	39
5	MeGE	2000:4:4	100	98	>99	27.2 (1.11)	40
6	MeGE	2000:2:2	95	98	>99	29.6 (1.12)	41

Reaction conditions: Co(Salen)Cl as a catalyst and [PPN]Cl as an initiator, monomer (1 mL), 50 bar CO<sub>2</sub>, r.t., 24 hours. <sup>a</sup>[m]<sub>0</sub> = monomer equivalents, [i]<sub>0</sub> = initiator equivalents, [cat]<sub>0</sub> = catalyst equivalents. <sup>b</sup>Determined *via* <sup>1</sup>H NMR spectroscopy from the non-purified reaction mixture after opening the reactor; conv. = epoxide conversion determined *via* comparison of the relative integrals in the <sup>1</sup>H NMR spectrum of PC, CC, PE, and monomer. <sup>c</sup>Determined *via* <sup>1</sup>H NMR spectrum from the non-purified reaction mixture after opening the reactor; select. = polymer selectivity determined *via* comparison of the relative integrals in the <sup>1</sup>H NMR spectrum for PC against CC. <sup>d</sup>Determined *via* comparison of the relative integrals in the <sup>1</sup>H NMR spectrum for PC against PE. <sup>e</sup>Determined *via* SEC (THF, PS) and RI detector.



to a maximum of 57%. The content of polycarbonate linkages notably impacts the  $T_g$  values in the MeGE based polycarbonate, resulting in a  $T_g$  range from 0 to 41 °C with 0% or 100% content of polycarbonate linkages in the final polymer (see ESI Fig. S30†). Overall, the Co(Salen)Cl catalytic system showed superior polymerization performance considering both polymer selectivity and content of polycarbonate linkages compared to the TEB catalytic system for the monomers MeGE and ThyGE.

### Polymer properties

The three presented terpene-based polycarbonates exhibit similar structures, of which the structures based on thymol and carvacrol are even constitutional isomers. While the copolymerization performance of each monomer is similar, they show significant differences in their polymer properties. When examining similar molar masses, PThyGEC displays the highest  $T_g$  at 58 °C, PMeGEC shows the lowest  $T_g$  at 41 °C, while PCarGEC ranged in between with 49 °C (see Fig. 3A). One key observation is the impact of  $\pi$ - $\pi$  stacking on the  $T_g$  for PCarGEC and PThyGEC, whereas polycarbonates derived from MeGE possess lower  $T_g$  values due to absence of this additional interaction. According to literature, the presence of  $\pi$ - $\pi$  stacking leads to an increase of the  $T_g$ .<sup>28</sup>

Surprisingly, the  $T_g$  difference between PThyGEC and PCarGEC is almost 10 K, despite the only distinction being the position of the methyl/isopropyl group at the phenyl ring. This suggests that PThyGEC might have a more tightly packed chain structure, while PCarGEC's isopropyl chains contribute to plasticizing the polymer structure. The position of the isopropyl/methyl group in PCarGEC and PThyGEC significantly influences the glass transition. Nonetheless, all three polymers exhibit lower  $T_g$  values compared to polycarbonates where the cyclic structure is part of the polymer backbone, such as poly(cyclohexene oxide) carbonate (PCHC) ( $T_g$  = 118 °C), PLimC ( $T_g$  = 130 °C), or PMen2C ( $T_g$  = 144 °C).<sup>14</sup> The presence of the "glycidyl ether spacer" obviously results in a less rigid polymer

structure, leading to lower  $T_g$ . This effect is particularly noticeable when comparing PMeGEC with PMen2C, where the  $T_g$  difference exceeds 100 °C. In addition, the thermal degradation for each polymer shows differences (see Fig. 3B). While PThyGEC and PCarGEC exhibit nearly identical  $T_{5\%}$  values at 260 °C, PMeGEC exhibits a lower  $T_{5\%}$  at 221 °C when comparing similar molar masses. When comparing the  $T_{5\%}$  values of pure menthol and thymol, thymol shows also a higher  $T_{5\%}$ .<sup>60</sup> In comparison to PLimC ( $T_{5\%}$  = 229 °C), PCarGEC and PThyGEC exhibit higher thermal stability, but are surpassed by PCHC ( $T_{5\%}$  = 283 °C), and PMen2C ( $T_{5\%}$  = 308 °C).<sup>18</sup>

Tensile testing of PCarGEC, PThyGEC, and PMeGEC samples has also been carried out. All polymers showed promising film-forming properties when solvent casting from chloroform and annealing at 100 °C. However, specific challenges arose for PMeGEC: the film was non-processable at lower temperatures due to high brittleness, while at room temperature, it became sticky (see ESI Fig. S33A†). This characteristic results from its  $T_g$  close to room temperature. PCarGEC showed successful film formation, but exhibited significant brittleness when punched into the dog bone shape, causing the film to shutter (see ESI Fig. S33B†). Consequently, conducting tensile testing was not feasible. PThyGEC displayed good film-forming properties (see ESI Fig. S33C†). Upon manual bending, the resulting films exhibited high flexibility (see ESI Fig. S34†). Comparing all three polycarbonates, it becomes evident that not only the  $T_g$  value plays a crucial role, but also the side chains.

All PThyGEC tensile tests were conducted from the reuse of the same polymer batch (after tensile testing, dissolving polymer and subsequent film generation), highlighting its reprocessability. The films show no direct failure after reaching their stress maximum displaying some elastic deformation. This phenomenon may stem from the slow flow of polymer chains, influenced by weak chain entanglements and interactions. The films demonstrate a Young's modulus ( $E$ ) of  $645 \pm 43$  MPa and an elongation at break ( $\epsilon$ ) of  $5 \pm 2\%$ , both at

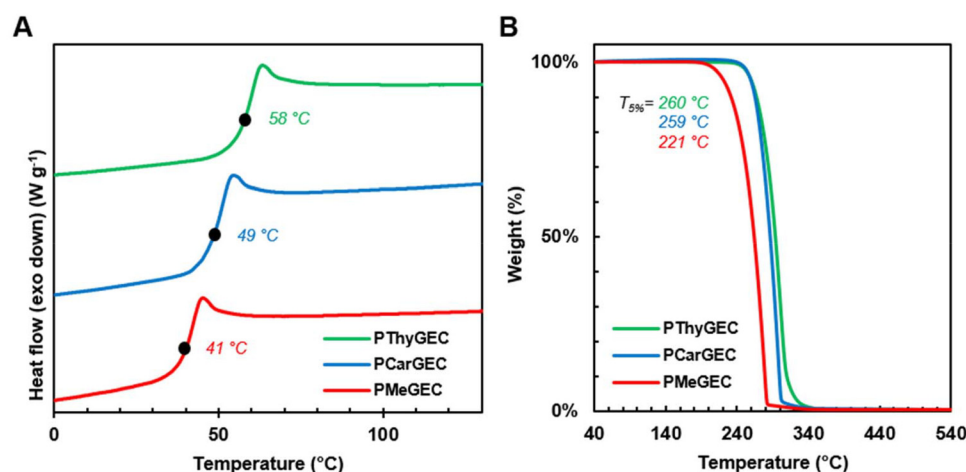
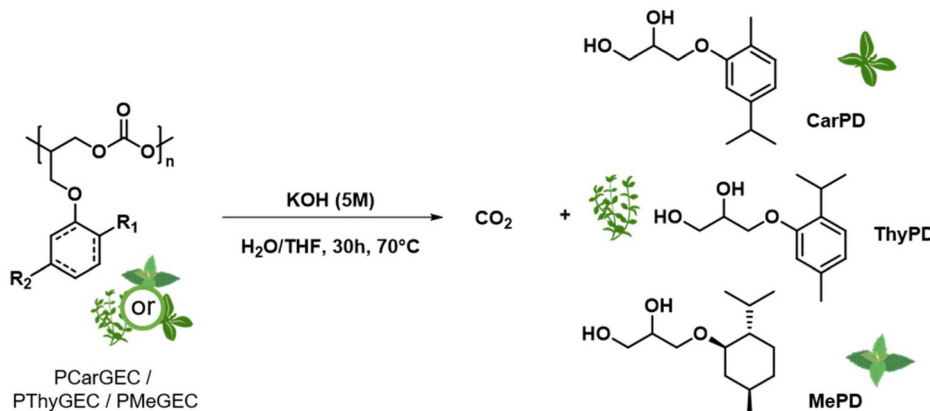


Fig. 3 (A) DSC measurements and (B) TGA measurements of the three different terpenoid-based copolymers.





Scheme 2 Polymer degradation of PCarGEC, PThyGEC and PMeGEC to terpene-based diols.

ambient temperature. The elongation at break falls within a similar range as that of PCHC.<sup>61</sup> Comparing the Young's modulus, PThyGEC falls in a similar range as PPC.<sup>61</sup> However, the higher  $T_g$  of PThyGEC compared to PPC ( $T_g = 20\text{--}40\text{ }^\circ\text{C}$ ) is a significant advantage. In contrast to PCHC, PThyGEC exhibits a lower Young's modulus, most probably due to the absence of a cyclic structure in the polymer backbone.<sup>61</sup>

### Polymer degradation

The degradation of  $\text{CO}_2$ -based polycarbonates can result in the formation of cyclic carbonates, epoxides, or diols depending on the chosen conditions.<sup>41,46,62</sup> Under different degradation conditions and depending on the monomer type, degradation can occur gradually over several weeks or rapidly within a few hours. Ideally, these degradation products can be utilized or polymerized thereafter or are metabolized by microorganisms in soil. Terpenes find wide application in medicine or for general biomedical purposes, either in their original form or as tailored derivatives for specific purposes.<sup>63</sup> For instance, thymol, carvacrol, and menthol have a range of pharmaceutical applications with many different derivatives used.<sup>64–66</sup> Hence, our objective for the presented polycarbonates was to obtain degradation products that are applicable for subsequent use. To focus on the degradation products rather than the degradation process itself, we selected harsh conditions to achieve full degradation. All three polymers, PCarGEC ( $M_n = 20.5\text{ kg mol}^{-1}$ ), PThyGEC ( $M_n = 21.5\text{ kg mol}^{-1}$ ), PMeGEC ( $M_n = 16.7\text{ kg mol}^{-1}$ ) were treated with an  $\text{H}_2\text{O}/\text{THF KOH (5 M)}$  solution for 30 hours at  $70\text{ }^\circ\text{C}$  (see Scheme 2). All three experiments showed complete degradation of the respective polymer, and no evidence of the polymer was detectable by SEC analysis and  $^1\text{H}$  NMR characterization. Three different degradation product combinations are theoretically possible: epoxide monomer &  $\text{CO}_2$ , cyclic carbonate, or diol &  $\text{CO}_2$ . However, only the pure diol was observable *via*  $^1\text{H}$  NMR and  $^{13}\text{C}$  NMR characterization (see ESI Fig. S12–S18 and S32†) with all signals assigned and no additional side products. Even if the cyclic carbonate or the epoxide are formed, they would

undergo direct conversion into diols due the harsh basic conditions. The pure isolated diols are white solids in the case of CarPD and ThyPD, and a liquid for MePD.

While the terpene derivative diols have a similar terpene scent compared to their alcohol counterparts, the intensity is notably suppressed. Regarding circularity, although these diols are not reusable as monomers for copolymerization with  $\text{CO}_2$ , they hold promising application possibilities. MePD, commercially known as agent 10, and its derivatives, for instance, exhibit potential use as effective cooling agents, surpassing other methanol combinations.<sup>67</sup> Thymol and carvacrol derivatives with a similar structure to ThyPD and CarPD find applications as drug candidates or metabolic enzyme inhibitors,<sup>68</sup> while thymol and carvacrol themselves are extensively employed in disease treatment like cancer or cardiometabolic diseases.<sup>64,66</sup> Consequently, ThyPD and CarPD might exhibit similar properties or serve as precursors for more complex thymol/carvacrol-based structures. Overall, thermal recycling offers a promising opportunity to extend the lifespan of the presented polymers, avoiding chemical down cycling issues, instead creating low molecular products for alternative secondary applications without the need of any further purification. The bioactivity of the polymers and their degradation products are in focus of future investigations.

### Conclusions

Biobased polycarbonates, derived from cyclic terpenoid-based glycidyl ethers and  $\text{CO}_2$ , have been introduced. Utilizing a  $\text{Co}(\text{Salen})\text{Cl}/[\text{PPN}]\text{Cl}$  catalytic system, all three epoxides based on menthol, carvacrol and thymol, were successfully copolymerized with  $\text{CO}_2$  within 24 hours at room temperature. We achieved molar masses up to  $60\text{ kg mol}^{-1}$ , with low dispersities confirmed by SEC (THF, PS). The molar masses can be controlled by initiator concentration or by the addition of chain transfer agents (CTAs). Notably, the absolute molar mass determined by universal calibration was found to be up to 18% higher due to the systematic underestimation of the side



chains in the SEC (THF, PS). Transitioning to a TEB/[PPN]Cl catalytic system, recognized for its metal-free and eco-friendly nature, copolymerization was also possible. In this case, precise optimization of the catalyst ratios was necessary to attain high polymer selectivity and polycarbonate linkages. The properties of the novel polycarbonates are highly influenced by the terpene structure of the glycidyl ether monomer. A  $T_g$  range between 41 to 58 °C was achieved, while polymers with the potential for  $\pi$ - $\pi$  stacking in their side chains exhibited higher  $T_g$  values (PCarGEC and PThyGEC). This distinction was also evident in the thermal degradation experiments, as polymers with  $\pi$ -system in their side chain reached  $T_{5\%}$  of 260 °C. Tensile testing was only successful for PThyGEC samples, demonstrating a high Young's modulus of 645 MPa and low flexibility. Investigating degradation possibilities, all polymers underwent degradation under strong basic conditions, yielding the respective diols and CO<sub>2</sub>. Considering the polymers' end-of-life usage, CO<sub>2</sub> is reusable in polycarbonate production and the diols may further serve as raw materials in the cosmetic and pharmaceutical industries.

## Author contributions

The manuscript was written through contributions of all authors. All authors have given approval to the final version of the manuscript.

## Data availability

The data supporting this article have been included as part of the ESI.†

## Conflicts of interest

There are no conflicts to declare.

## Acknowledgements

The authors want to thank the Max-Planck-Institute for Polymer Research in Mainz and especially Petra Räder for measuring the TGA of all polymers.

## References

- United Nations, *Africa Renewal*, 2015, **29**, 8.
- M. Stafford-Smith, D. Griggs, O. Gaffney, F. Ullah, B. Reyers, N. Kanie, B. Stigson, P. Shrivastava, M. Leach and D. O'Connell, *Sustainability Sci.*, 2017, **12**, 911–919.
- Polymers, Biopolymer-Based Materials towards the Sustainable Development Goals, available at: [https://www.mdpi.com/journal/polymers/special\\_issues/8RII9XX1S7](https://www.mdpi.com/journal/polymers/special_issues/8RII9XX1S7), accessed 02/2024.
- D. Kyriacos, *Brydson's Plastics Materials*, Butterworth-Heinemann, Oxford, 8th edn, 2017.
- J. Maia, J. M. Cruz, R. Sendón, J. Bustos, J. J. Sanchez and P. Paseiro, *Food Res. Int.*, 2009, **42**, 1410–1414.
- (a) Y. Liu and X.-B. Lu, *Macromolecules*, 2023, **56**, 1759–1777; (b) P. Wei, G. A. Bhat and D. J. Darenbourg, *Angew. Chem.*, 2023, **135**, e202307507; (c) G. A. Bhat and D. J. Darenbourg, *Green Chem.*, 2022, **24**, 5007–5034; (d) S. Paul, Y. Zhu, C. Romain, R. Brooks, P. K. Saini and C. K. Williams, *Chem. Commun.*, 2015, **51**, 6459–6479.
- Y.-Y. Zhang, G.-P. Wu and D. J. Darenbourg, *Trends Chem.*, 2020, **2**, 750–763.
- X. Li, L. Meng, Y. Zhang, Z. Qin, L. Meng, C. Li and M. Liu, *Polymers*, 2022, **14**, 2159.
- (a) M. M. Halmann and M. Steinberg, *Greenhouse gas carbon dioxide mitigation*. Science and Technology, Boca Raton, FL, 1999; (b) T. Ema, *Bull. Chem. Soc. Jpn.*, 2023, **96**, 693–701.
- M. Sengoden, G. A. Bhat and D. J. Darenbourg, *Macromolecules*, 2023, **56**, 2362–2369.
- D. K. Tran, A. Z. Rashad, D. J. Darenbourg and K. L. Wooley, *Polym. Chem.*, 2021, **12**, 5271–5278.
- J. Yang, J. Dong, Y. Wang, X. Zhang, B. Liu, H. Shi and L. He, *Macromolecules*, 2021, **54**, 8503–8511.
- S. Cui, Y. Qin and Y. Li, *ACS Sustainable Chem. Eng.*, 2017, **5**, 9014–9022.
- F. Della Monica and A. W. Kleij, *Polym. Chem.*, 2020, **11**, 5109–5127.
- O. Hauenstein, M. Reiter, S. Agarwal, B. Rieger and A. Greiner, *Green Chem.*, 2016, **18**, 760–770.
- (a) F. Parrino, A. Fidalgo, L. Palmisano, L. M. Ilharco, M. Pagliaro and R. Ciriminna, *ACS Omega*, 2018, **3**, 4884–4890; (b) C. Martín and A. W. Kleij, *Macromolecules*, 2016, **49**, 6285–6295; (c) L. P. Carrodeguas, T. T. D. Chen, G. L. Gregory, G. S. Sulley and C. K. Williams, *Green Chem.*, 2020, **22**, 8298–8307; (d) C. Li, M. Johansson, P. Buijsen, G. Dijkstra, R. J. Sablong and C. E. Koning, *Prog. Org. Coat.*, 2021, **151**, 106073; (e) S. Kernbichl and B. Rieger, *Polymer*, 2020, **205**, 122667; (f) C. M. Byrne, S. D. Allen, E. B. Lobkovsky and G. W. Coates, *J. Am. Chem. Soc.*, 2004, **126**, 11404–11405; (g) C. Li, R. J. Sablong and C. E. Koning, *Eur. Polym. J.*, 2015, **67**, 449–458; (h) C. Li, R. J. Sablong and C. E. Koning, *Angew. Chem., Int. Ed.*, 2016, **55**, 11572–11576.
- O. Hauenstein, S. Agarwal and A. Greiner, *Nat. Commun.*, 2016, **7**, 11862.
- A. Wambach, S. Agarwal and A. Greiner, *ACS Sustainable Chem. Eng.*, 2020, **8**, 14690–14693.
- (a) Y. Zhi, X. Shan, S. Shan, Q. Jia, Y. Ni and G. Zeng, *J. CO2 Util.*, 2017, **22**, 299–306; (b) W. Fan, Q. Jia, J. Mu and S. Shan, *China Pat.*, CN103333329A, 2015.
- S. Schüttner, C. Gardiner, F. S. Petrov, N. Fotaras, J. Preis, G. Floudas and H. Frey, *Macromolecules*, 2023, **56**, 8247–8259.
- P. Holzmüller, C. Gardiner, J. Preis and H. Frey, *Macromolecules*, 2024, **57**, 5358–5367.



22 (a) G. Shukla and R. C. Ferrier, *J. Polym. Sci.*, 2021, **59**, 2704–2718; (b) A. Almena and M. Martín, *Ind. Eng. Chem. Res.*, 2016, **55**, 3226–3238; (c) K. Weissermel and H.-J. Arpe, *Industrial Organic Chemistry*, Wiley-VCH, Weinheim, 3rd edn, 2008.

23 B. M. Bell, J. R. Briggs, R. M. Campbell, S. M. Chambers, P. D. Gaarenstroom, J. G. Hippler, B. D. Hook, K. Kearns, J. M. Kenney, W. J. Kruper, D. J. Schreck, C. N. Theriault and C. P. Wolfe, *Clean: Soil, Air, Water*, 2008, **36**, 657–661.

24 P. Krafft, P. Gilbeau and B. Gosselin, *US Pat.*, US9663427B2, 2017.

25 P. Krafft, P. Gilbeau, B. Gosselin and S. Claessens, *US Pat.*, US2009/0270588 AI, 2009.

26 D. Cespi, R. Cucciniello, M. Ricciardi, C. Capacchione, I. Vassura, F. Passarini and A. Proto, *Green Chem.*, 2016, **18**, 4559–4570.

27 (a) J. Degenhardt, T. G. Köllner and J. Gershenzon, *Phytochemistry*, 2009, **70**, 1621–1637; (b) C.-Q. Yang, X.-M. Wu, J.-X. Ruan, W.-L. Hu, Y.-B. Mao, X.-Y. Chen and L.-J. Wang, *Phytochemistry*, 2013, **96**, 46–56.

28 H. T. H. Nguyen, P. Qi, M. Rostagno, A. Feteha and S. A. Miller, *J. Mater. Chem. A*, 2018, **6**, 9298–9331.

29 J. Baranauskaitė, V. Jakštė, L. Ivanauskas, D. M. Kopustinskienė, G. Drakšienė, R. Masteikova and J. Bernatoniene, *Nat. Prod. Res.*, 2016, **30**, 672–674.

30 D. Villanueva Bermejo, I. Angelov, G. Vicente, R. P. Stateva, M. Rodriguez García-Risco, G. Reglero, E. Ibañez and T. Fornari, *J. Sci. Food Agric.*, 2015, **95**, 2901–2907.

31 I. Batool, S. Nisar, L. Hamrouni and M. I. Jilani, *Int. J. Chem. Biomol. Sci.*, 2018, **14**, 71–76.

32 (a) S. E. Aly, A. S. Hathout and N. A. Abo-Sereih, *J. Biol. Act. Prod. Nat.*, 2011, **1**, 293–305; (b) G.-W. Zheng, J. Pan, H.-L. Yu, M.-T. Ngo-Thi, C.-X. Li and J.-H. Xu, *J. Biotechnol.*, 2010, **150**, 108–114.

33 (a) A. Marchese, I. E. Orhan, M. Daglia, R. Barbieri, A. Di Lorenzo, S. F. Nabavi, O. Gortzi, M. Izadi and S. M. Nabavi, *Food Chem.*, 2016, **210**, 402–414; (b) V. V. M. A. Souza, J. M. Almeida, L. N. Barbosa and N. C. C. Silva, *J. Essent. Oil Res.*, 2022, **34**, 181–194; (c) J. A. Farco and O. Grundmann, *Mini-Rev. Med. Chem.*, 2013, **13**, 124–131; (d) M. Sharifi-Rad, E. M. Varoni, M. Iriti, M. Martorell, W. N. Setzer, M. Del Mar Contreras, B. Salehi, A. Soltani-Nejad, S. Rajabi, M. Tajbakhsh and J. Sharifi-Rad, *Phytother. Res.*, 2018, **32**, 1675–1687; (e) N. B. Rathod, P. Kulawik, F. Ozogul, J. M. Regenstein and Y. Ozogul, *Trends Food Sci. Technol.*, 2021, **116**, 733–748.

34 (a) V. H. Campos-Querena, B. L. Rivas, M. A. Pérez, C. R. Figueroa and E. A. Sanfuentes, *LWT – Food Sci. Technol.*, 2015, **64**, 390–396; (b) E. Sanchez-Rexach, I. Martínez de Arenaza, J.-R. Sarasua and E. Meaurio, *Eur. Polym. J.*, 2016, **83**, 288–299; (c) N. Petchwattana and P. Naknaen, *Mater. Chem. Phys.*, 2015, **163**, 369–375; (d) R. Requena, M. Vargas and A. Chiralt, *Food Hydrocolloids*, 2018, **83**, 118–133; (e) R. Scaffaro, A. Maio, E. F. Gulino, M. Morreale and F. P. La Mantia, *Materials*, 2020, **13**, 983; (f) A. Sansukcharearnpon, S. Wanichwecharungruang, N. Leepipatpaiboon, T. Kerdcharoen and S. Arayachukeat, *Int. J. Pharm.*, 2010, **391**, 267–273.

35 (a) M. Winnacker, S. Vagin, V. Auer and B. Rieger, *Macromol. Chem. Phys.*, 2014, **215**, 1654–1660; (b) M. Winnacker, A. Tischner, M. Neumeier and B. Rieger, *RSC Adv.*, 2015, **5**, 77699–77705.

36 (a) W. T. Diment, G. Rossetto, N. Ezaz-Nikpay, R. W. F. Kerr and C. K. Williams, *Green Chem.*, 2023, **25**, 2262–2267; (b) J. Shin, Y. Lee, W. B. Tolman and M. A. Hillmyer, *Biomacromolecules*, 2012, **13**, 3833–3840.

37 (a) S. Bedel, B. Lepoittevin, L. Costa, O. Leroy, D. Dragoe, J. Bruzaud, J.-M. Herry, M. Guilbaud, M.-N. Bellon-Fontaine and P. Roger, *J. Polym. Sci., Part A: Polym. Chem.*, 2015, **53**, 1975–1985; (b) E. H. Min, K. H. Wong, E. Setijadi, F. Ladouceur, M. Stratton and A. Argyros, *Polym. Chem.*, 2011, **2**, 2045.

38 K. M. Mydeen, J. P. Kanth, A. Hariharan, K. Balaji, S. Rameshkumar, G. Rathika and M. Alagar, *J. Polym. Environ.*, 2022, **30**, 5301–5312.

39 G. A. Parolin, L. F. D. Passero, J. H. G. Lago and L. O. Péres, *Ind. Crops Prod.*, 2021, **171**, 113935.

40 (a) I. A. Ignatyev, W. Thielemans and B. Vander Beke, *ChemSusChem*, 2014, **7**, 1579–1593; (b) M. Grigore, *Recycling*, 2017, **2**, 24; (c) V. M. Pathak and B. Navneet, *Bioresour. Bioprocess.*, 2017, **4**, 15; (d) N. Lucas, C. Bienaime, C. Belloy, M. Queneudec, F. Silvestre and J.-E. Nava-Saucedo, *Chemosphere*, 2008, **73**, 429–442.

41 F. Siragusa, C. Detrembleur and B. Grignard, *Polym. Chem.*, 2023, **14**, 1164–1183.

42 (a) A. Beharaj, E. Z. McCaslin, W. A. Blessing and M. W. Grinstaff, *Nat. Commun.*, 2019, **10**, 5478; (b) F.-T. Tsai, Y. Wang and D. J. Daresbourg, *J. Am. Chem. Soc.*, 2016, **138**, 4626–4633.

43 K. D. Knight and M. E. Fieser, *Inorg. Chem. Front.*, 2023, **11**, 298–309.

44 (a) P. P. Pescarmona, *Curr. Opin. Green Sustainable Chem.*, 2021, **29**, 100457; (b) C.-C. Su, M. He, R. Amine, Z. Chen, R. Sahore, N. Dietz Rago and K. Amine, *Energy Storage Mater.*, 2019, **17**, 284–292.

45 (a) G. W. Coates and Y. D. Y. L. Getzler, *Nat. Rev. Mater.*, 2020, **5**, 501–516; (b) M. L. Smith, T. M. McGuire, A. Buchard and C. K. Williams, *ACS Catal.*, 2023, **24**, 15770–15778; (c) G. Rossetto, F. Vidal, T. M. McGuire, R. W. F. Kerr and C. K. Williams, *J. Am. Chem. Soc.*, 2024, **146**, 8381–8393.

46 F. N. Singer, A. C. Deacy, T. M. McGuire, C. K. Williams and A. Buchard, *Angew. Chem.*, 2022, **134**, e202201785.

47 (a) T. M. McGuire, A. C. Deacy, A. Buchard and C. K. Williams, *J. Am. Chem. Soc.*, 2022, **144**, 18444–18449; (b) Y. Yu, B. Gao, Y. Liu and X.-B. Lu, *Angew. Chem.*, 2022, **134**, e202204492.

48 (a) C. Li, R. J. Sablong, R. A. T. M. van Benthem and C. E. Koning, *ACS Macro Lett.*, 2017, **6**, 684–688; (b) D. Ghosh and S. Agarwal, *Polym. Chem.*, 2023, **14**, 4626–4635; (c) D. H. Lamparelli, A. Villar-Yanez, L. Dittrich,



J. Rintjema, F. Bravo, C. Bo and A. W. Kleij, *Angew. Chem., Int. Ed.*, 2023, **62**, e202314659.

49 B. Liu, J. Chen, N. Liu, H. Ding, X. Wu, B. Dai and I. Kim, *Green Chem.*, 2020, **22**, 5742–5750.

50 A. Akira, H. Toshimitsu, M. Takashi and A. Teruyoshi, *Japanese Pat.*, JP20010124134, 2002.

51 (a) D. J. Daresbourg, *Chem. Rev.*, 2007, **107**, 2388–2410; (b) M. Scharfenberg, J. Hilf and H. Frey, *Adv. Funct. Mater.*, 2018, **28**, 1704302.

52 Z. Qin, C. M. Thomas, S. Lee and G. W. Coates, *Angew. Chem., Int. Ed.*, 2003, **42**, 5484–5487.

53 C. T. Cohen, T. Chu and G. W. Coates, *J. Am. Chem. Soc.*, 2005, **127**, 10869–10878.

54 (a) D. J. Daresbourg, *J. Chem. Educ.*, 2017, **94**, 1691–1695; (b) G.-P. Wu and D. J. Daresbourg, *Macromolecules*, 2016, **49**, 807–814.

55 M. R. Ambler, *J. Polym. Sci., Polym. Chem. Ed.*, 1973, **11**, 191–201.

56 C. T. Cohen and G. W. Coates, *J. Polym. Sci., Part A: Polym. Chem.*, 2006, **44**, 5182–5191.

57 C. Earl, I. H. Shah, S. Cook and C. R. Cheeseman, *Sustainability*, 2022, **14**, 4124.

58 (a) D.-D. Zhang, X. Feng, Y. Gnanou and K.-W. Huang, *Macromolecules*, 2018, **51**, 5600–5607; (b) D. Zhang, S. K. Boopathi, N. Hadjichristidis, Y. Gnanou and X. Feng, *J. Am. Chem. Soc.*, 2016, **138**, 11117–11120.

59 Z. Chen, J.-L. Yang, X.-Y. Lu, L.-F. Hu, X.-H. Cao, G.-P. Wu and X.-H. Zhang, *Polym. Chem.*, 2019, **10**, 3621–3628.

60 M. Trivedi, S. Patil, R. Mishra and S. Jana, *J. Mol. Pharm. Org. Process Res.*, 2015, **03**, 1000127.

61 *Engineering solutions for CO<sub>2</sub> conversion*, ed. T. R. Reina, J. A. Odriozola and H. Arellano-Garcia, Wiley-VCH, John Wiley & Sons, Inc., Weinheim, Hoboken, NJ, 2021.

62 (a) J. K. Varghese, S. J. Na, J. H. Park, D. Woo, I. Yang and B. Y. Lee, *Polym. Degrad. Stab.*, 2010, **95**, 1039–1044; (b) Y. Yu, B. Gao, Y. Liu and X.-B. Lu, *Angew. Chem.*, 2022, **134**, e202204492.

63 (a) M. Jahangeer, R. Fatima, M. Ashiq, A. Basharat, S. A. Qamar, M. Bilal and H. M. Iqbal, *J. Pure Appl. Microbiol.*, 2021, **15**, 471–483; (b) S. D. Tetali, *Planta*, 2019, **249**, 1–8.

64 M. F. Nagoor Meeran, H. Javed, H. Al Taee, S. Azimullah and S. K. Ojha, *Front. Pharmacol.*, 2017, **8**, 380.

65 G. P. P. Kamatou, I. Vermaak, A. M. Viljoen and B. M. Lawrence, *Phytochemistry*, 2013, **96**, 15–25.

66 K. H. C. Baser, *Curr. Pharm. Des.*, 2008, **14**, 3106–3119.

67 (a) C. Fuganti, D. Joulain, F. Maggioni, L. Malpezzi, S. Serra and A. Vecchione, *Tetrahedron: Asymmetry*, 2008, **19**, 2425–2437; (b) A. Yokohama, M. Mitaka and T. Yokohama, *US Pat.*, 4459425, 1984; (c) A. O. Barel, M. Paye and H. I. Maibach, *Cooling Ingredients and Their Mechanism of Action*, Informa Healthcare, New York, N.Y., 2009; (d) R. Eccles, *J. Pharm. Pharmacol.*, 1994, **46**, 618–630; (e) M. Fujii, Y. Takeda, M. Yoshida, N. Utoguchi, M. Matsumoto and Y. Watanabe, *Int. J. Pharm.*, 2003, **258**, 217–223.

68 (a) A. Bytyqi-Damoni, A. Kestane, P. Taslimi, B. Tuzun, M. Zengin, H. G. Bilgieli and İ. Gulcin, *J. Mol. Struct.*, 2020, **1202**, 127297; (b) M. Zengin, H. Genc, P. Taslimi, A. Kestane, E. Guclu, A. O gutlu, O. Karabay and İ. Gulçin, *Bioorg. Chem.*, 2018, **81**, 119–126.

